

The Transient Friction Response of a Laser-Textured, Reciprocating Contact to the Entrainment of Individual Pockets

Sorin-Cristian Vlădescu¹ · Simon Medina¹ · Andrew V. Olver¹ · Ian G. Pegg² · Tom Reddyhoff¹

Received: 14 December 2015 / Accepted: 14 March 2016 / Published online: 25 March 2016
© The Author(s) 2016. This article is published with open access at Springerlink.com

Abstract To shed light on the mechanisms with which surface texture improves the tribological performance of piston–liner contacts, we have measured the transient friction response as individual pockets pass through a reciprocating sliding contact. Tests were performed at different sliding speeds and results compared to those from a non-textured, reference specimen under different lubrication regimes. At low speed when the contact is in the boundary regime, friction force falls abruptly as each pocket leaves the contact zone, before gradually returning to an approximately steady-state value. This suggests that each pocket acts to temporarily increase the film thickness, which then decays to its non-textured value as oil is squeezed out. At higher speeds, friction is seen to reduce in a stepwise fashion, since the period between pockets being entrained is less than the time taken for the film to decay. In addition, friction results obtained when the contact is operating in the middle of the mixed regime point to a temporary film thickness collapse as the pocket enters the contact, and this agrees with recent modelling predictions. At higher speeds, the compound effect of successive pockets is to shift the contact to the right on Stribeck curve. These results imply that each pocket gives rise to an increase in film thickness that is both short-lived and small in magnitude (we estimate a few tens of nm). However, the resulting effect on friction can be significant (up to 82 % in

this study) for two reasons: (1) provided the pocket frequency is sufficiently high, each successive pocket entrainment builds the film up without there being time for it to reduce back to its steady-state value; (2) when the contact is in the mixed regime, the Stribeck curve is at its steepest and friction is therefore most sensitive to film thickness changes. This has important practical implications in that pocket spacing on piston liners should be varied as a function of reciprocating sliding speed.

Keywords Surface texture · Friction reduction · Piston rings · Transient lubrication

1 Introduction

Increasingly strict CO₂ emission standards, as well as a persistent rise in crude oil prices, have led motor vehicle manufacturers to seek ways of improving IC engine efficiency. An obvious strategy is to tackle engine friction losses since studies show these constitute a significant proportion (11.5 %) of the dissipated fuel energy, of which the piston/cylinder system accounts for 45 % [1]. For instance, as stated by Korcek et al. [2] and Macian et al. [3], the use of low viscosity oils (LVOs) is increasingly being embraced by OEMs. This is done in order to reduce hydrodynamic losses and lower the engine power, required to achieve a specific set of operating conditions. The disadvantage of this approach is that mixed and boundary lubrication conditions are becoming increasingly prevalent in IC engines. For instance, the piston–bore contact is being pushed towards mixed and boundary lubrication conditions along a significantly increased length of its reciprocating stroke, whereas it was originally understood to operate under such conditions only in the vicinity of the

✉ Sorin-Cristian Vlădescu
s.vlădescu12@imperial.ac.uk

¹ Tribology Group, Department of Mechanical Engineering, Imperial College London, South Kensington Campus, Exhibition Road, London SW7 2AZ, UK

² Ford Motor Company, Dunton, Essex, UK

two dead centres (with hydrodynamic prevailing at mid-stroke [4]).

Another, complementary and more localised, method that may reduce friction is to apply laser surface texturing (also referred to as laser honing or LST) to engine components, particularly the ring–liner pairing.

Over the last decade, researchers at Imperial College compared the performance of a wide range of texture geometries, under various operating scenarios, in both experimental and theoretical studies [5–10]. Recently, the group’s experiments showed that, under reciprocating piston–liner type conditions, beneficial or detrimental effects of surface texture could be achieved depending on which lubrication regime the contact operated under [9]. Specifically, it was concluded that surface texture can reduce friction in low film thickness contacts, whereas it increased friction in the full-film lubrication regime. Furthermore, latest results show that this effect on friction is due to surface texture’s ability to increase or decrease lubricant film thickness [10].

Etsion et al. [11–18] also contributed to the field through a range of insightful experimental observations. Notably, they demonstrated the importance of aspect ratio and other co-dependent geometric parameters used to describe a textured pattern in controlling the friction performance of a microtextured bearing. Following this, Fowell et al. [7] and Medina et al. [8] developed numerical techniques to assess the effectiveness of, and interdependency between, texture parameters.

Further valuable experimental work was carried out by Costa and Hutchings [19] to investigate tribological behaviour of surfaces with differently shaped pockets. After measuring film thickness in the reciprocating contact using a capacitance technique, they concluded that the addition of certain patterns can increase film thickness at given loads. A further notable observation, in agreement with experimental measurements, reported by the current authors [9] and Petterson and Jacobson [20], was that pockets parallel to the direction of sliding result in higher friction and lower film thickness.

These studies demonstrated that applying texture to surfaces can have both beneficial and detrimental effects on tribological performance. In the former cases, various micro-textured patterns, applied to bearing surfaces, afforded increased load support or greater film thickness. However, these findings are of limited practical benefit, since the majority of experimental work to date has been restricted to hydrodynamically lubricated bearings under steady-state conditions. Transient effects, caused by individual texture features passing through the contact, have largely been overlooked, as has the interaction between texture and both squeeze film and Stribeck behaviour. As a result, there remains uncertainty regarding the exact

mechanisms, by which surface texture controls friction, despite several speculated hypotheses that are summarised below.

In 1966, Hamilton and Allen conducted a pioneering study of textured bearings [21, 22], introducing the concept of “micro-irregularities” and suggesting that surface texture can create resistance that acts to prevent fluid from escaping the contact. Following this, Tønder [23, 24] proposed that surface patterns generate a “virtual step”, within the contact that resembles the discontinuous change in film thickness associated with Rayleigh step bearings. Later, when studying the behaviour of transverse roughness in EHL lubricated contacts, Morales-Espejel [25] and Greenwood and Morales-Espejel [26] suggested that each asperity peak entering contact zone behaves as a flow exciter that closes and opens the inlet to allow varying amounts of fluid to enter. This phenomenon is possible since both pressure and roughness deformations are low in the vicinity of the inlet. Years later, Morales-Espejel et al. [27] highlighted another possible phenomenon associated with surface texture that may affect load support and consequently friction force. They observed that, under EHL lubrication conditions, oil is released from the pocket under pressure as a result of elastic deformation of the material in the contact area. In 2006, the concept of “inlet suction” was identified in Olver and Fowell’s work [7], whereby the reduction in pressure afforded by cavitation as lubricant expands into a pocket at the contact inlet leads to an increase in lubricant entrainment and hence film thickness. Most recently, while investigating cavitation behaviour in a reciprocating contact using laser-induced fluorescence (LIF), the authors of this paper observed a reduction in oil entrainment (starvation) upon reversal possibly due to the cavitated region, under mixed and boundary lubrication conditions. As pockets bring lubricant into the cavitated region, they may aid entrainment and as a result reduce friction under these conditions.

In summary, the correct application of surface texture leads to significant reductions in friction particularly in the mixed and boundary regime, and this may have practically useful applications in IC engine contacts. In addition to this, a number of highly insightful mechanisms have been proposed to account for such behaviour. However, almost none of these mechanisms (i.e. those described above) have been supported by direct experimental evidence. The need for experimental validation of surface texture effects is most needed in the mixed regime where few, if any, comparisons have been made between theory and measurements. To address this, the current study aims to shed light on the mechanisms by which surface pockets cause an increase in film thickness by observing the transient friction response as individual pockets pass through a sliding contact. The specific conditions are chosen to simulate

closely those found in a piston ring–liner pairing, operating in the boundary or mixed lubrication regimes.

2 Experimental Details

A reciprocating test rig was designed with the specific purpose of measuring frictional response under conditions that replicate those in a piston ring–liner pairing; the main limitation of the test apparatus is the use of a single ring (simulating the top ring), as opposed to the three or more piston rings comprising the actual cylinder configuration. The stroke length and sliding speeds used in these tests also differ from those found in an actual engine; however, this is necessary in order to make the observations that we require (other studies have conducted experiments at higher speeds sliding speeds, e.g. [28] et al.; however, these have not shed light on the transient effects due to the entrainment of individual pockets).

The experimental rig, described in detail in [9], uses a low-capacity isometric load cell to measure the friction force between a flat fused silica plate, representing the cylinder liner, and a 2-mm-wide convex AISI52100 steel pad, representing the piston ring. The 10-mm-long steel pad is curved in the direction of sliding to ensure a convergent–divergent bearing geometry. An adjustable stroke cam mechanism is employed to control the reciprocal motion of the fused silica specimen relative to the fixed steel pad. The pad specimen holder was designed to allow for the displacement of the two steel shims away from or towards the load cell, onto which it is directly coupled.

The key to this experimental approach, schematically presented in Fig. 1, is that all experimental conditions are controlled with a high degree of accuracy. For instance, since the most critical parameter for accurate comparisons between plain and textured surfaces is oil temperature, a carefully designed oil supply system was built on the

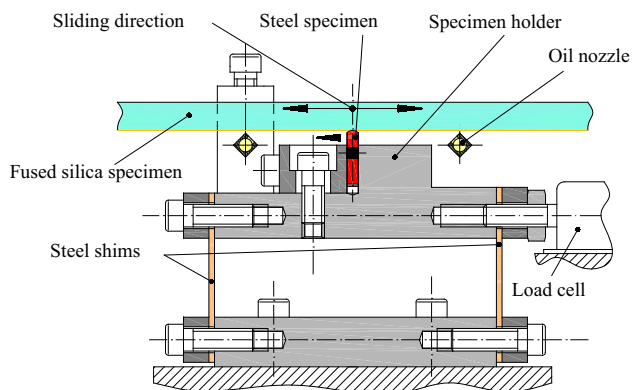


Fig. 1 Schematic representation of the experimental set-up for measuring the friction in a reciprocating contact

reciprocating sliding rig. This consisted of an immersion circulator, a gear pump transporting oil to the contact zone and a peristaltic pump returning it to the circulator, and as a result, the lubricant is fed to the contact with a stability of 0.2 °C, at any chosen temperature between +10 and +150 °C.

The effects of pockets in reciprocating sliding bearings were investigated by employing two fused silica specimens—an untextured and a textured one (Fig. 2). Rectangular grooves, with an orientation normal to the direction of sliding, were chosen, since these have been proven effective in decreasing friction force by up to 62 % when compared to the non-textured reference [9]. These pockets, which were 1 mm in length, 80 μm in breadth, 8 μm deep and spaced at 3.3 mm, were etched using a laser, having an optical pulse duration of 10 picoseconds. The 3.3 mm separation between each line of pockets was specifically selected so that the effect on friction force of individual pockets could be observed as they passed through the contact. A higher pocket density would result in a friction signal in which individual pockets could not be distinguished, while a sparser spacing would not allow compound of effect of subsequent pockets to be observed. Both the textured and non-textured fused silica rectangular pads have the same outer dimensions: 125 × 15 × 5 mm.

The counterpart ring specimen, initially a fully hardened (850 HV) AISI52100 rectangular steel pad with 10 × 10 × 2 mm outer dimensions, was ground on the 2 mm width side to a 40 mm radius (Fig. 3a). Following the grinding, a mirror-polished convex surface was achieved along the length of the pad using a specially designed polishing jig (Fig. 3b). To ensure correct loading along the length of the contact, when switching between the textured and the non-textured fused silica specimens, the steel pad is fitted with a self-aligning mechanism. This consisted of a hole, through which a 4-mm-diameter pin was positioned with a +80 μm tolerance, and resulted in a continuous self-adjustment with the counterpart silica specimen.

Tests were carried out using a stroke length of 28.6 mm, under a normal load of 70 N, applied using dead weights at one end of the silica pad holder. Throughout the entire testing programme, the same fully formulated engine oil was used with its temperature, and hence viscosity, being accurately maintained at the values shown in Table 1.

3 Results and Discussion

3.1 Repeatability

Before studying the transient effect of pockets, the reliability of the test set-up was assessed. To do this, repeat tests

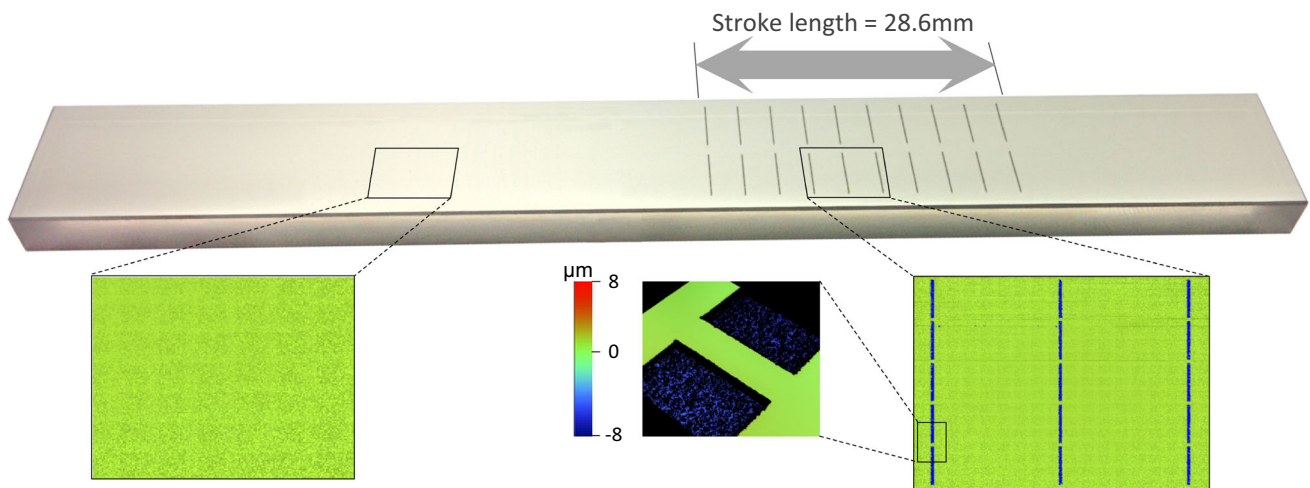


Fig. 2 Surface topography of the textured and untextured fused silica specimens as obtained by the Veeco Wyko NT9100 optical profiler

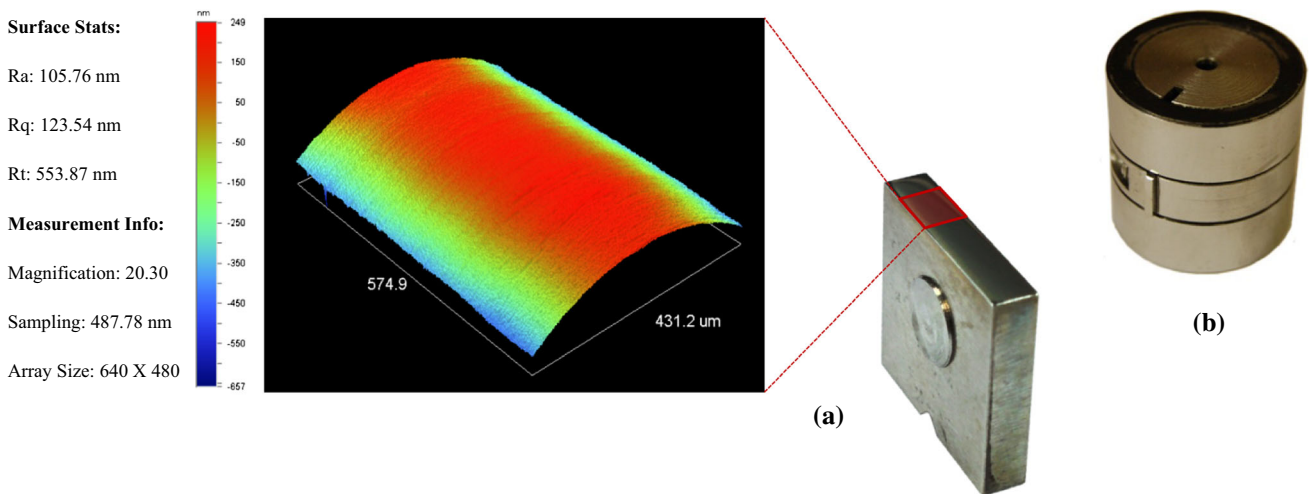


Fig. 3 **a** Three-dimensional surface profile of the convergent–divergent steel specimen; **b** Polishing jig

Table 1 Properties of the fully engine-formulated lubricant at the desired temperatures selected for this study

Oil temperature [°C]	Oil properties		
	Dynamic viscosity η [mPa s]	Kinematic viscosity ν [mm ² /s]	Density ρ [g/cm ³]
10.0	401.350	460.264	0.8720
80.0	18.847	22.753	0.8283

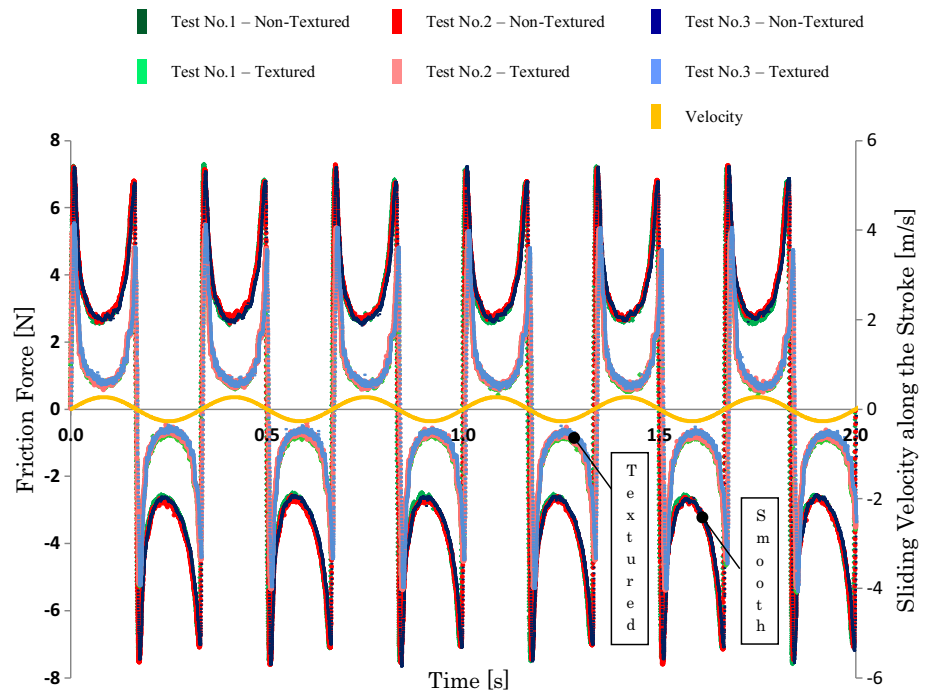
were carried out under a single combination of test conditions, for both non-textured and textured silica specimens (crank angular velocity: 3 Hz, normal load: 50 N, oil viscosity: 18.8 mPa s). The variation of friction force, both over time and between different days (while switching between specimens), was tested. The results in Fig. 4 show there is negligible variation in results over time. The figure also shows that the contact is operating in mixed/boundary lubrication conditions due to the reduction in

friction with increasing speed. In addition to this, the substantial reduction in friction, caused by the presence of surface pockets, is evident.

3.2 Overall Steady-State Friction Response

Transient friction tests were performed under the sets of conditions shown in Table 2, producing the series of friction versus crank angle plots, presented in Sects. 3.3 and 3.4.

Fig. 4 Friction force versus time for both the specimens tested in this study (measurements obtained on different days). Test conditions: crank angular velocity: 3 Hz, normal load: 50 N, oil temperature: 80 °C



The use of two significantly different lubricant viscosities and a wide range of speeds meant that the lubrication regime, in which the contact operated, varied from boundary to mixed to full film. Therefore, before interpreting these results, it is useful to identify in which lubrication regime the contact was operating for during each test. This is done by fitting the friction data onto a single Stribeck master curve, as shown in Fig. 5. To achieve this, friction coefficient is plotted against speed \times viscosity for both plain and textured specimens, using that same data that is later shown in Figs. 6, 7 and 8. As explained previously [9], squeeze film effects were eliminated by selecting only friction data from crank angles between 40° and 140°. The plot shows how the presence of texture has the effect of shifting the Stribeck curve to the left and reduces friction in the mixed regime by as much as 82 %.

Note that the leftward shift in the Stribeck curve shown in Fig. 5 is in agreement with several previous studies of surface texture [29–31]. There are, however, other studies that show texture reducing friction in the full-film regime [19, 32, 33]. The unexplained discrepancies between these studies demonstrate that the effect of lubricant regime on

surface texture is not fully understood and requires more investigation.

3.3 Transient Response of Friction to Pockets in the Boundary and Mixed Lubrication Regimes

Figures 6 and 7 present the variation in friction force along a single stroke for the plain and the textured silica specimen, respectively, both at a constant oil temperature of 80 °C (oil viscosity: 18.8 mPa s). Under these conditions, the contact is operating predominantly in boundary and mixed conditions.

In Fig. 7, the friction force variation can be observed for the textured specimen with crank angular velocities between 0.15 and 5 Hz at 80 °C. It should be noted that, since Fig. 7 shows friction force versus crank angle, the length of time associated with each plot reduces as the angular velocity increases (e.g. at 0.15 Hz it takes 3.33 s to travel 180°, while at 5 Hz it takes 0.1 s). Despite some noise in the signal, caused by fluctuations in load, it is immediately noticeable that individual pockets produce various transient effects on friction as they pass through the contact area. For crank angular speeds of 0.15 and 0.3 Hz, friction force is reduced when pockets pass; however, the opposite occurs when the speed is between 0.6 and 3 Hz, with individual pockets temporarily increasing friction force. Lastly, when the angular speed is increased to 5 Hz, the features passing through contact have no significant local effect on frictional response.

Table 2 Complete set of test conditions

Load W [N]	Oil temperature [°C]	Crank angular velocity [Hz]					
70	10.0	–	0.3	0.6	1	3	5
	80.0	0.15	0.3	0.6	1	3	5

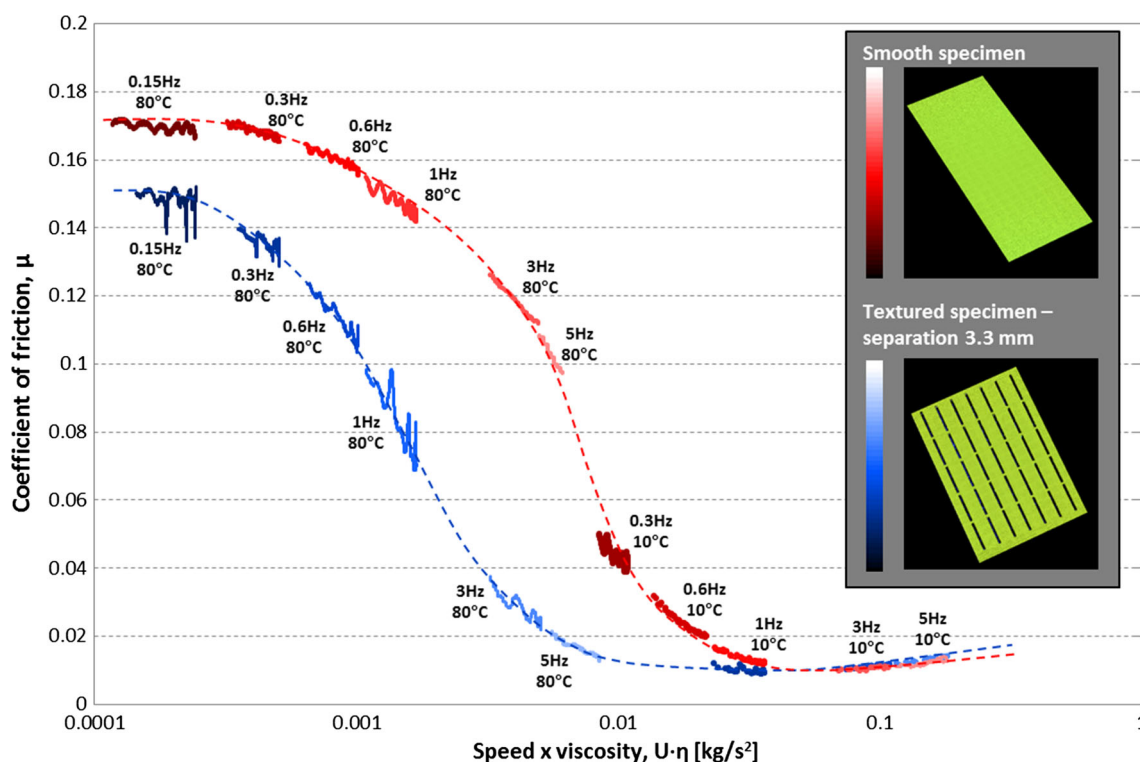


Fig. 5 Stribeck curves showing friction behaviour for the two fused silica specimens used in this study

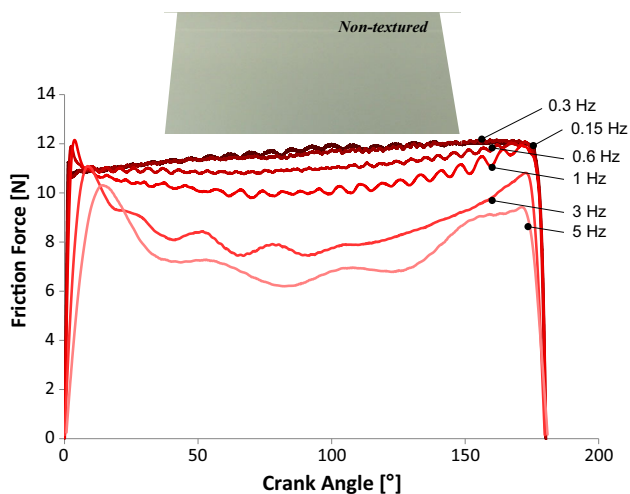


Fig. 6 Friction force comparison between different crank angular velocities—non-textured specimen (test conditions: normal load: 70 N, oil temperature: 80 °C)

From Fig. 7a, it can be seen that, while running in the boundary lubrication regime (0.15 Hz crank angular velocity, 80 °C), friction force decreases abruptly as soon as a pocket leaves the contact, before gradually returning to its initial value (F_0). This behaviour is in agreement with previous findings by the current authors [10] which showed that textured features act to increase lubricant entrainment

into the contact, and hence reduces asperity friction. It then follows that the subsequent gradual increase in friction can be attributed to the oil film being steadily squeezed out of the contact. This mechanism results in a friction force that repeatedly returns to a constant maximum value along the entire stroke. The corresponding results for the non-textured case (the 0.15 Hz angular velocity plot in Fig. 6) show a friction force value that, at the beginning of the stroke, is similar to that of the textured specimen. However, the non-textured frictional response then increases continuously throughout the stroke, reaching its maximum close to the reversal point. This behaviour of the non-textured specimen has also been observed by previous researchers [34, 35] and in this case demonstrates the beneficial effect of texture in relieving friction build-up.

Further analysis of the textured specimen’s frictional response (Fig. 7—Detail B) reveals that, at a crank angular velocity of 0.3 Hz, the bearing has shifted from the boundary lubrication regime towards the initial part of the mixed regime (Fig. 5). The same friction reduction characteristics as the 0.15 Hz case are observed, i.e. a rapid reduction in friction that coincides as each pocket enters the contact followed by a gradual increase. However, at this velocity, the period of time between pockets entering contact is half that of the 0.15 Hz case, and therefore, the friction force does not have time to return to its initial value (F_0) before the next pocket arrives. A stepwise reduction in

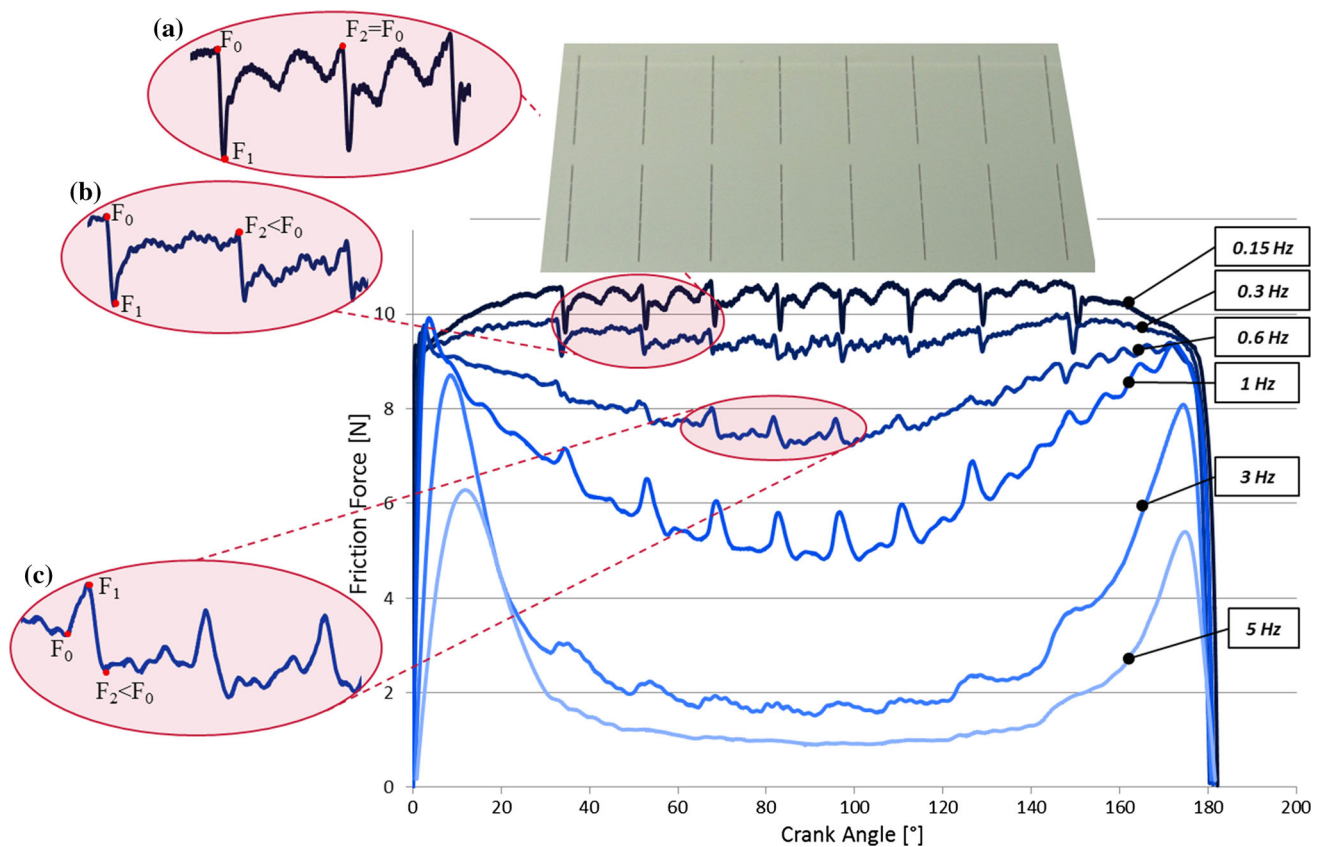


Fig. 7 Friction force measurements for various crank angular velocities, using the textured fused silica specimen (normal load 70 N, oil viscosity: 18.8 mPa s)

friction is thus observed, with a minimum value at mid-stroke. The “downward steps” until mid-stroke, followed by the “upward steps” for the remainder of the stroke, are correlated with the approximately sinusoidal sliding speed that reaches its peak mid-stroke. By comparison, the plain specimen, tested under the same load and angular velocity, remains in the boundary lubrication regime throughout the entire stroke, with no change in friction force between 0.15 and 0.3 Hz.

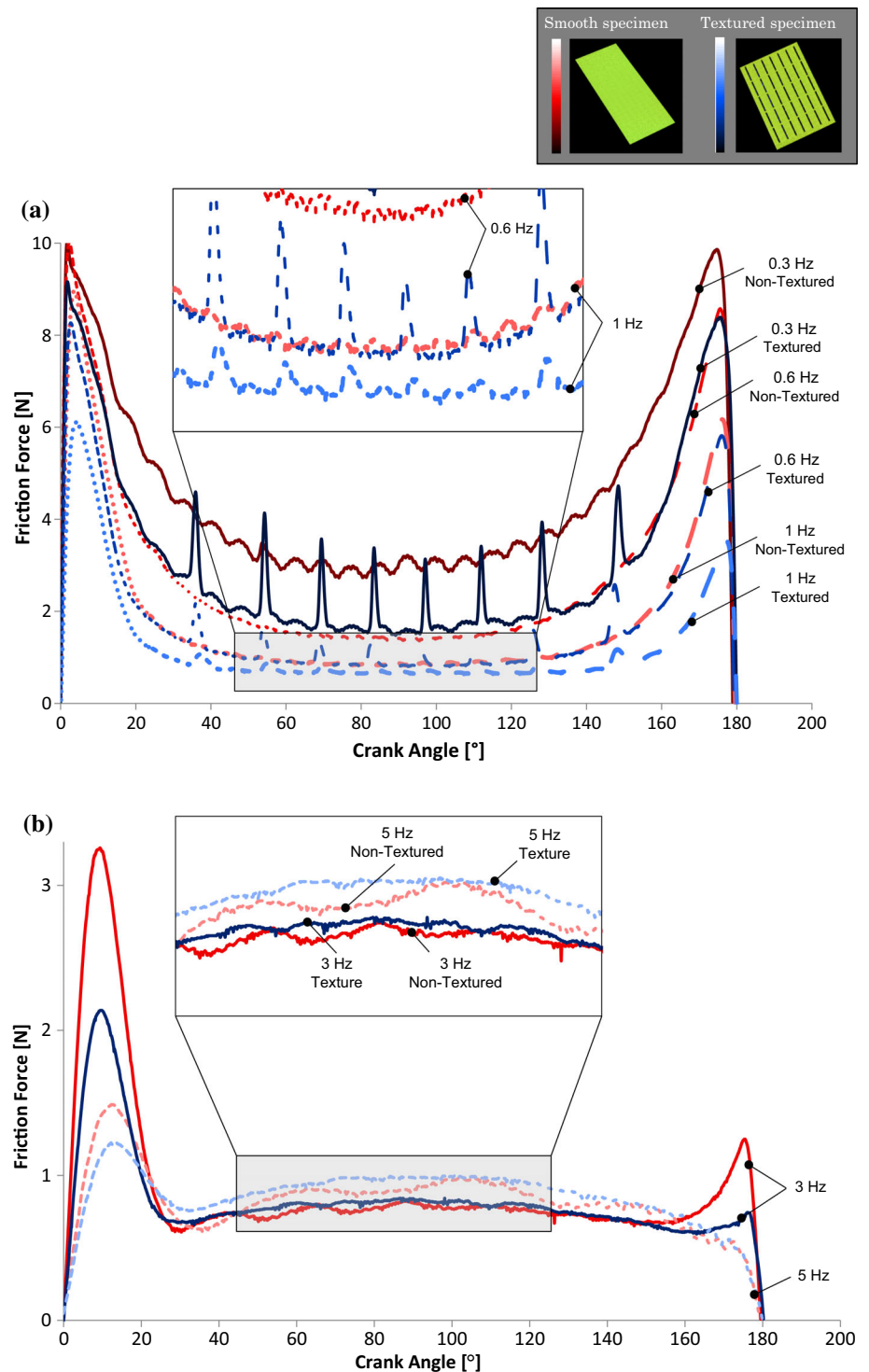
For angular velocities of 0.6 and 1 Hz, a different transient variation in friction is observed with the textured silica specimen (Fig. 7—Detail C). As soon as the pocket enters contact, the friction force increases from F_0 to F_1 . Then, as the pocket leaves the contact, the friction force descends to a value F_2 , which is lower than the initial value F_0 . The step-like behaviour is preserved throughout the stroke, but, in contrast to the boundary lubrication case, the instantaneous friction force does not reduce until the pocket leaves the sliding contact. When comparing the plain and textured bearing under these conditions, it is obvious that the latter is already midway through the mixed lubrication regime (for a crank angular velocity of 1 Hz), whereas the former has hardly left the boundary regime.

This transient friction peak that is observed is likely to be caused by an instantaneous collapse of the oil film due to the order of magnitude reduction in contact area as the pocket is entrained. This leaves the ring specimen momentarily in contact with the area surrounding the pocket, before the action of the pocket leaving the contact boosts film thickness.

This peak is not noticeable at lower speeds, most probably due to the plateauing of the Stribeck curve (i.e. at very low speeds there is no oil film to collapse). The difference in friction between the plain and textured bearings increases further at higher speeds, when the latter is operating on the steepest region of the Stribeck curve. In this case, reductions of up to 82 % are recorded when friction from the textured specimen is compared to that of the plain reference specimen for a crank angular velocity of 5 Hz. Another interesting observation is that the transient effect of individual pockets on friction gradually disappears as the contact approaches the full-film regime (i.e. the conditions under which friction is insensitive to changes in film thickness).

In the boundary and mixed regime, an overall transient response to pocket entrainment that can be inferred from

Fig. 8 Friction force comparison between textured and non-textured samples for various crank angular velocities: **a** 0.3, 0.6 and 1 Hz; **b** 3 and 5 Hz (test conditions: oil viscosity: 401.350 mPa s; normal load 70 N)



the above results is (1) film thickness decrease due to contact area reduction, followed by (2) film thickness increase, followed by (3) decay due to squeeze action—a process which agrees qualitatively with recent modelling predictions of load support variation during pocket entrainment [8]. This process is suggested based on the fact that the measured variations in friction result from changes in film thickness.

This is justified by a recent experimental study (using the same set-up as this one) by the current authors, which demonstrated that the friction reduction due to presence of surface texture in the mixed lubrication regime does indeed result from an increase in film thickness [10].

Additional effects on friction response can be observed when comparing the textured specimen with the plain

reference. Firstly, in many cases, the textured specimen shows lower friction than the non-textured case, even before the textured region reaches the contact (e.g. friction traces, at 3 Hz, between 10 and 30°). This difference may in part be due to the action of the texture bringing lubricant into the cavitated region, to prevent starvation at reversal (as suggested by [36]). However, it is also likely to be caused by difference in squeeze film thickness at reversal between the two cases—i.e. the compound effect of multiple pocket entrainments builds a thicker film that is more persistent at reversal so that, when the speed subsequently increases, the contact slides further down the Stribeck curve.

Comparing the friction variation along the first 30° of crank angle in Figs. 6 (non-textured specimen) and 7 (textured specimen) suggests that pockets should be placed immediately before/after reversal in an actual piston–liner to achieve the beneficial effects described above. However, as previously demonstrated, textured features should not be located exactly at the reversal point as these acts collapse the oil film [9].

3.4 Transient Response of Friction to Pockets in the Mixed and Full-Film Lubrication Regimes

Figure 8 shows the relationship between friction force and crank angle for the same specimens, at a constant oil temperature of 10 °C (oil viscosity: 401.3 mPa s)—conditions which favour mixed to full-film conditions.

When the bearing is operating in the mixed regime, close to the bottom of the Stribeck curve, the friction reduction due to pocket entrainment becomes less pronounced. This is shown in Fig. 8a and is consistent with previous observations [9]. The friction spike, attributed to film collapse as the contact moves over the pocket, is again evident (Fig. 8a—0.3 and 0.6 Hz) and has a high magnitude due to the gradient of Stribeck curve, in this region (i.e. there is an appreciable film for the pocket to collapse). At higher speeds (1 Hz), the effect on friction of individual pockets becomes indistinct. This is due to a combination of factors including the flattening of the Stribeck curve in this region and possibly the reduction in the time each pocket covers the contact.

When the bearing is in the full-film lubrication regime (Fig. 8b), the smooth specimen begins to outperform the laser surface-textured one, exhibiting lower friction forces along the entire stroke. As observed in Fig. 8b (for test velocity: 3, 5 Hz), the difference between the two samples (now with the non-textured sample showing lowest friction) increases as the speed increases and the contact is moved towards the right of the master Stribeck curves. As shown in a recent study [10], the increase in friction in the

full-film regime can be attributed to texture causing a reduction in film thickness.

3.5 Estimation of Film Thickness Variation that Results from Pocket Entrainment

Based on the friction data from this study, it is possible to estimate the approximate film thickness variation that results from a single pocket entrainment, using the following steps. First, the film thickness for the non-textured contact is calculated for the range of speeds and viscosities tested, by applying Hamrock's Equations (once the correct elastohydrodynamic lubricant regime was established). The calculated film thickness is then plotted against the corresponding measured steady-state friction data (i.e. the Stribeck data in Fig. 5) and a polynomial curve fitted. This polynomial function can then be applied to the friction on data measured for the textured case to estimate the corresponding film thickness. This relies on both textured and non-textured contacts having the same dependence of friction on film thickness as has been demonstrated previously [10]. Applying this method to the friction variation from Fig. 7b results in the film thickness plot shown in Fig. 9. Here, it can be seen that the pocket causes an increase in film thickness of a few tens of nanometres (which then reduces as it is squeezed from the contact). This is in agreement with film thickness measurements for multiple pocket entrainments, which under the same conditions show increases of ~20 nm [10]. It is likely that this variation in film thickness and friction will depend on the viscosity of the lubricant (i.e. higher viscosity lubricants

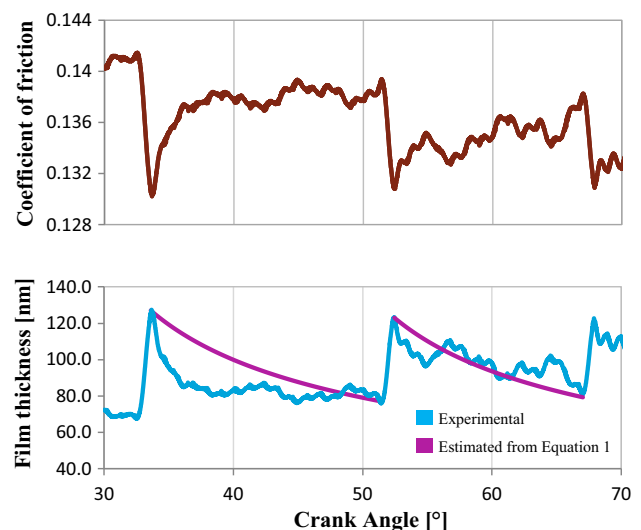


Fig. 9 Coefficient of friction variation along the stroke and corresponding estimated film thickness for oil viscosity: 18.8 mPa s reciprocating speed of 0.3 Hz and applied load: 70 N

will take longer to be squeezed out and will therefore) and is the subject of further study.

To test the hypothesis that the observed variation in friction between pocket entrainments is due to oil being squeezed from the contact, these experimental results can be compared with a very approximate calculation of squeeze film thickness. Assuming a Barus pressure–viscosity relationship at that the sliding speed is sufficiently low so as to make lubricant entrainment negligible, then Reynolds' Equation for an infinitely long rectangular pad can be integrated to give the variation in squeeze film thickness with crank angle, φ :

$$h(\varphi) = \left(\frac{2W}{\eta_0 e^{\alpha p} B^3} \left(\frac{\varphi + \varphi_0}{f} \right) + \frac{1}{h_0^2} \right)^{-1/2} \quad (1)$$

where W is the applied load (70 N), η_0 is the viscosity at atmospheric pressure (18.8 mPa s), f is the reciprocating frequency (0.3 Hz), B is the Hertzian width of the contact (160 μm), α is the pressure viscosity coefficient (16 GPa^{-1}), φ_0 and h_0 are the crank angle and the film thickness when the pocket leaves the contact (33.6° and 127 μm , respectively).

Equation (1) is plotted alongside the experimental data in Fig. 9, where it can be seen that there is a surprisingly good agreement with the variation in measured film thickness (both methods show reductions in film thickness of a similar order). This goes some way to suggest that the variation in friction between pockets is indeed due to squeeze film effects; however, it should be noted that this is an extremely approximate analysis, which assumes a simplified geometry and ignores the effect of asperity stiffness. A more exacting comparison between experiment and modelling is the focus of ongoing research.

4 Conclusions

A carefully designed reciprocating tribometer was used to obtain the transient friction response to pocket entrainment. The lubrication regime and pocket entrainment speed were precisely controlled, and results were compared to those from a non-textured specimen.

Laser surface texture applied on linear bearing surfaces is a powerful means of reducing friction under boundary and mixed lubrication conditions. This is demonstrated by improvements in friction performance of up to 82 %, when comparing the average stroke friction values from the textured and non-textured specimens. Conversely, in the full-film regime, texture causes a slight increase in friction. These effects manifest themselves as a leftward shift of the Stribeck curve and are indicative of enhanced/reduced fluid

film thickness. The transient response to individual pocket entrainments can be summarised as follows:

- In the mixed and boundary regimes, sliding speed has a strong effect on texture performance via two routes. Firstly, the speed determines where on the Stribeck curve the contact is operating and therefore how sensitive the friction force is to changes in film thickness. Secondly, the speed controls the pocket entrainment frequency and hence determines whether the film thickness has time decay to its steady-state value between pocket entrainments. This also has important practical implications regarding the configuration of pockets on piston liners, since the pocket entrainment frequency may be adjusted, according to the varying sliding speed, by gradating the geometric pocket spacing.
- In the boundary lubrication regime where the load is supported predominantly by asperity contact, a steep reduction in friction force is observed as each pocket leaves the contact, presumably due to an abrupt increase in film thickness.

If the pocket entrainment velocity is sufficiently low, there is time for this additional film to be squeezed out before the next pocket arrives. Although this does not result in a compound reduction in friction, pocket entrainment under these conditions prevents a gradual build-up in friction force as is observed with the non-textured pad.

At higher pocket entrainment speeds, the contact does not have time to recover from subsequent pocket entrainments, and as a result, the friction reduces in a stepwise fashion (see Fig. 10a, b).

- Under mixed lubrication conditions, where the load is supported by a combination of lubricant pressure and asperity contact, the transient friction response shows a peak value as each pocket enters the contact (Fig. 10c). It is suggested that this is due to the considerable reduction in contact area as the pocket passes, and as a consequence, the lubricant film is believed to collapse. Even under these conditions, the net effect of pocket entrainment is still to increase lubricant thickness along the stroke and significantly reduce the friction below the non-textured case.
- When running at high pocket entrainment frequencies in the mixed regime, the effect of successive pockets entering the contact builds up. It is suggested that this causes a beneficial increase in film thickness that carries over to subsequent reciprocations by means of the squeeze film effect. This is supported by the fact that the friction for the textured specimen drops far more rapidly than for the plain specimen, at the start of

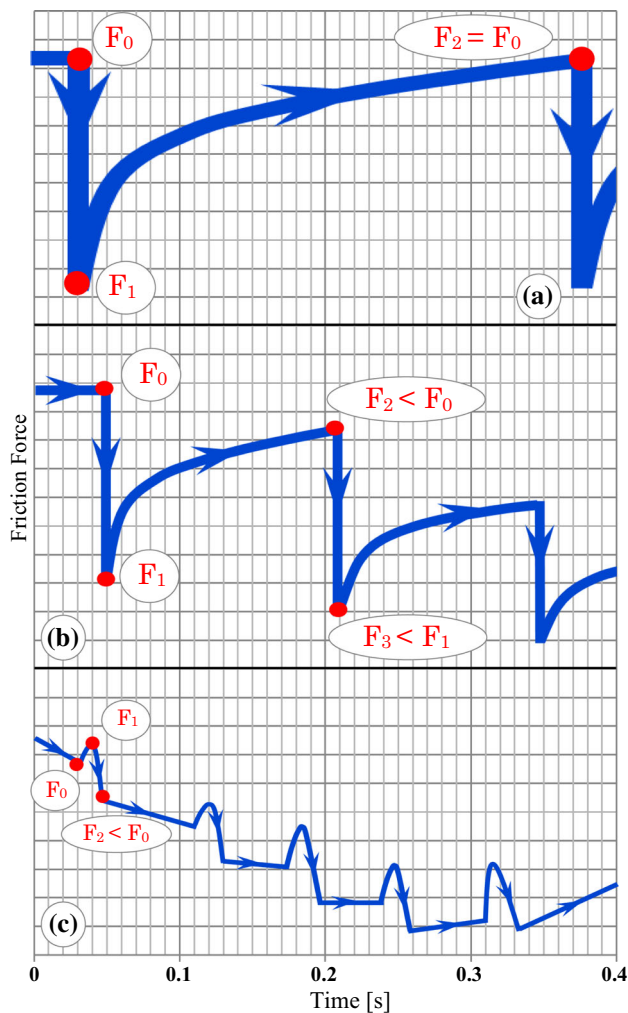


Fig. 10 Schematic representation of the transient effects of pockets passing through contact for different crank speeds: **a** 0.15 Hz; **b** 0.3 Hz; **c** 0.6 Hz

the reciprocation, before any pockets have entered the contact.

The transient friction and film thickness data, obtained by monitoring the entrainment of individual pockets in this way, are in qualitative agreement with recent numerical simulations (such as [8]) of sliding LST surfaces, and further comparison should help to elucidate the friction reduction mechanisms that are occurring.

Acknowledgments The authors are grateful to Khizer Tufail and Arup Gangopadhyay for their advice and support. The project was funded by the Ford Motor Company.

Open Access This article is distributed under the terms of the Creative Commons Attribution 4.0 International License (<http://creativecommons.org/licenses/by/4.0/>), which permits unrestricted use, distribution, and reproduction in any medium, provided you give appropriate credit to the original author(s) and the source, provide a

link to the Creative Commons license, and indicate if changes were made.

References

- Holmberg, K., Andersson, P., Erdemir, A.: Global energy consumption due to friction in passenger cars. *Tribol. Int.* **47**, 221–234 (2012)
- Korcek, S., Sorab, J., Johnson, M.D., Jensen, R.K.: Automotive lubricants for the next millennium. *Ind. Lubr. Tribol.* **52**, 209–220 (2000)
- Macián, V., Tormos, B., Bermúdez, V., Ramírez, L.: Assessment of the effect of low viscosity oils usage on a light duty diesel engine fuel consumption in stationary and transient conditions. *Tribol. Int.* **79**, 132–139 (2014)
- Gore, M., King, P.D., Howell-Smith, S., Rahnejat, H.: Measurement of in-cylinder friction using the floating liner principle. In: *Proceedings on ASME 2012 Internal Combustion Engine Division Spring Technical Conference*, pp. 1–6 (2012)
- Olver, A.V., Fowell, M.T., Spikes, H.A., Pegg, I.G.: “Inlet suction”, a load support mechanism in non-convergent, pocketed, hydrodynamic bearings. *Proc. Inst. Mech. Eng., Part J: J. Eng. Tribol.* **220**, 105–108 (2006)
- Fowell, M., Olver, A.V., Gosman, A.D., Spikes, H.A., Pegg, I.G.: Entrainment and inlet suction: two mechanisms of hydrodynamic lubrication in textured bearings. *J. Tribol.* **129**, 336–347 (2007)
- Fowell, M.T., Medina, S., Olver, A.V., Spikes, H.A., Pegg, I.G.: Parametric study of texturing in convergent bearings. *Tribol. Int.* **52**, 7–16 (2012)
- Medina, S., Fowell, M.T., Vlădescu, S.-C., Reddyhoff, T., Pegg, I., Olver, A.V., Dini, D.: Transient effects in lubricated textured bearings. *Proc. Inst. Mech. Eng., Part J: J. Eng. Tribol.* **229**, 523–537 (2015)
- Vlădescu, S.-C., Olver, A.V., Pegg, I.G., Reddyhoff, T.: The effects of surface texture in reciprocating contacts—an experimental study. *Tribol. Int.* **82**, 28–42 (2015)
- Vlădescu, S.-C., Medina, S., Olver, A.V., Pegg, I.G., Reddyhoff, T.: Lubricant film thickness and friction force measurements in a laser surface textured reciprocating line contact simulating the piston ring—liner pairing. *Tribol. Int.* **98**, 317–329 (2016)
- Etsion, I., Kligerman, Y., Halperin, G.: Analytical and experimental investigation of laser-textured mechanical seal faces. *Tribol. Trans.* **42**, 511–516 (1999)
- Ronen, A., Etsion, I., Kligerman, Y.: Friction-reducing surface-texturing in reciprocating automotive components. *Tribol. Trans.* **44**, 359–366 (2001)
- Kligerman, Y., Etsion, I., Shinkarenko, A.: Improving tribological performance of piston rings by partial surface texturing. *J. Tribol.* **127**, 632–638 (2005)
- Etsion, I.: State of the art in laser surface texturing. *J. Tribol.* **127**, 248 (2005)
- Ryk, G., Etsion, I.: Testing piston rings with partial laser surface texturing for friction reduction. *Wear* **261**, 792–796 (2006)
- Ryk, G., Kligerman, Y., Etsion, I., Shinkarenko, A.: Experimental investigation of partial laser surface texturing for piston-ring friction reduction. *Tribol. Trans.* **48**, 583–588 (2005)
- Etsion, I., Sher, E.: Improving fuel efficiency with laser surface textured piston rings. *Tribol. Int.* **42**, 542–547 (2009)
- Murthy, A.N., Etsion, I., Talke, F.E.: Analysis of surface textured air bearing sliders with rarefaction effects. *Tribol. Lett.* **28**, 251–261 (2007)
- Costa, H.L., Hutchings, I.M.: Hydrodynamic lubrication of textured steel surfaces under reciprocating sliding conditions. *Tribol. Int.* **40**, 1227–1238 (2007)

20. Pettersson, U., Jacobson, S.: Friction and wear properties of micro textured DLC coated surfaces in boundary lubricated sliding. *Tribol. Lett.* **17**, 553–559 (2004)
21. Hamilton, D.B., Walowit, J.A., Allen, C.M.: A theory of lubrication by micro-irregularities. *Trans. ASME J. Basic Eng.* **88**, 177–185 (1966)
22. Anno, J.N., Walowit, J.A., Allen, C.M.: Microasperity lubrication. *J. Lubr. Technol.* **90**, 351–355 (1968)
23. Tønder, K.: Dynamics of rough slider bearings: effects of one-sided roughness/waviness. *Tribol. Int.* **29**, 117–122 (1996)
24. Tønder, K.: Hydrodynamic effects of tailored inlet roughnesses: extended theory. *Tribol. Int.* **37**, 137–142 (2004)
25. Morales-Espejel, G.E.: Elastohydrodynamic lubrication of smooth and rough surfaces. Ph.D. Thesis, (1993)
26. Greenwood, J.A., Morales-Espejel, G.E.: The behaviour of transverse roughness in EHL contacts. *Proc. Inst. Mech. Eng., Part J: J. Eng. Tribol.* **208**, 121–132 (1994)
27. Morales-Espejel, G.E., Lugt, P.M., Van Kuilenburg, J., Tripp, J.H.: Effects of surface micro-geometry on the pressures and internal stresses of pure rolling EHL contacts. *Tribol. Trans.* **46**, 260–272 (2003)
28. Ryk, G., Kligerman, Y., Etsion, I.: Experimental investigation of laser surface texturing for reciprocating automotive components. *Tribol. Trans.* **45**, 444–449 (2002)
29. Kovalchenko, A., Ajayi, O., Erdemir, A., Fenske, G., Etsion, I.: The effect of laser surface texturing on transitions in lubrication regimes during unidirectional sliding contact. *Tribol. Int.* **38**, 219–225 (2005)
30. Braun, D., Greiner, C., Schneider, J., Gumbsch, P.: Efficiency of laser surface texturing in the reduction of friction under mixed lubrication. *Tribol. Int.* **77**, 142–147 (2014)
31. Borghi, A., Gualtieri, E., Marchetto, D., Moretti, L., Valeri, S.: Tribological effects of surface texturing on nitriding steel for high-performance engine applications. *Wear* **265**, 1046–1051 (2008)
32. Scaraggi, M., Mezzapesa, F.P., Carbone, G., Ancona, A., Tricarico, L.: Friction properties of lubricated laser-microtextured-surfaces: an experimental study from boundary- to hydrodynamic-lubrication. *Tribol. Lett.* **49**, 117–125 (2012)
33. Scaraggi, M., Mezzapesa, F.P., Carbone, G., Ancona, A., Sorgente, D., Lugarà, P.M.: Minimize friction of lubricated laser-microtextured-surfaces by tuning microholes depth. *Tribol. Int.* **75**, 123–127 (2014)
34. Wakuri, Y., Hamatake, T., Soejima, M., Kitahara, T.: Piston ring friction in internal combustion engines. *Tribol. Int.* **25**, 299–308 (1992)
35. Tateishi, Y.: Tribological issues in reducing piston ring friction losses. *Tribol. Int.* **27**, 17–23 (1994)
36. Chong, W.W.F., Teodorescu, M., Vaughan, N.D.: Cavitation induced starvation for piston-ring/liner tribological conjunction. *Tribol. Int.* **44**, 483–497 (2011)